# Quality of the rare earth aluminum borate crystals for laser applications, probed by high-resolution spectroscopy of the Yb³⁺ ion

K.N. Boldyrev [a,*], M.N. Popova [a], M. Bettinelli [b], V.L. Temerov [c], I.A. Gudim [c], L.N. Bezmaternykh [c], P. Loiseau [d], G. Aka [d], N.I. Leonyuk [e]

[a] Institute of Spectroscopy, RAS, 5 Fizicheskaya Street, Troitsk, Moscow Region 142190, Russia
[b] Department of Biotechnology, University of Verona and INSTM, UdR Verona, Ca'Vignal, Strada Le Grazie 15, Verona 37134, Italy
[c] Kirensky Institute of Physics, Siberian Branch of RAS, Krasnoyarsk 660036, Russia
[d] LCMCP-UMR CNRS 7574, ENSCP, 11 rue Pierre et Marie Curie, Paris 75005, France
[e] Moscow State University, Faculty of Geology, Vorobievy Gory, Moscow 119899, Russia

## ARTICLE INFO

## ABSTRACT

A comparative study was performed of the low-temperature high-resolution absorption spectra of the Yb³⁺ probe in $R_{1-x}Yb_xAl_3(BO_3)_4$ ($R$ = Y, Tm, Lu) crystals grown by flux technique independently in four different laboratories using different solvents. We show that the incorporation of solvent components into the crystal in the course of crystallization gives rise to spectral satellites of the Yb³⁺ $0(^2F_{7/2}) \rightarrow 0'(^2F_{5/2})$ absorption lines and assign particular satellites to the Yb³⁺ centers near the bismuth and molybdenum impurities (which decrease the transparency of YAB in the UV spectral range). We suggest this spectroscopic method for a rapid analysis of the quality of UV laser crystals and for improvement of growth technologies.

© 2012 Elsevier B.V. All rights reserved.

## 1. Introduction

YAl₃(BO₃)₄ (YAB) crystals are important nonlinear optical materials with a wide band gap [1,2]. Doped with the Nd³⁺ or Yb³⁺ ions, they are efficiently used in self-frequency doubling and self-frequency summing lasers [3–7]. YAB crystals codoped with Yb³⁺ and Tm³⁺ are promising for up-conversion lasers [8,9]. Undoped YAB crystals can be considered for the fourth harmonic generation of the Nd:YAG laser radiation.

Rare-earth aluminum borates melt incongruently, so the single crystals can be grown only from flux by lowering the temperature below the peritectic point. For this reason, it is very difficult to control growth defects, such as twinning, and uncontrollable impurities from the solvent. Such defects have a significant influence on the laser properties of the crystals. For example, the molybdenum impurity restricts the use of YAB crystals in the ultraviolet (UV) spectral range [10]. Therefore, the problem of impurity control and growth technique of YAB crystals deserves a serious investigation.

Recently, we have shown that the measurement of the fine structure of the zero-phonon $0(^2F_{7/2}) \rightarrow 0'(^2F_{5/2})$ absorption line of Yb³⁺ doped into a YAB crystal is a sensitive method for detecting uncontrollable impurities entering the crystal during the growth by a flux technique [11]. In the present work, we report on the high-resolution polarized low-temperature absorption spectra of various aluminum borates $R_{1-x}Yb_xAl_3(BO_3)_4$, ($R$ = Y, Tm, Lu) grown independently in different laboratories using different solvents and analyze uncontrollable impurities in these crystals by our spectroscopic method. Finally, we present data on the UV absorption edge in the YAB crystals under investigation.

## 2. Experiment

The $R_{1-x}Yb_xAl_3(BO_3)_4$ ($R$ = Y, Tm and Lu, $0 \leqslant x \leqslant 1$) single crystals were grown with the flux technique using different solvents. The majority of the crystals (**1–6** in Table 1) were grown in the Kirensky Institute of Physics (KIP) using a bismuth–lithium–molybdenum oxide solvent. The second group of YAB:Yb crystals was grown from flux based on potassium trimolybdate solvent. These crystals with different concentrations of Yb (the samples **7–11** in Table 1) were grown in three different laboratories, namely in the University of Verona (UV), in the Laboratory of Solid State Chemistry in Paris (LCMCP), and in the Moscow State University (MSU). The last group of YAB:Yb crystals was grown in LCMCP using LaB₃O₆ as the base for flux (sample **12** in Table 1).

**Table 1**

A list of the investigated samples. The used solvents and growth laboratories are indicated (see the text). Amount of the centers $Yb^{3+}(Mo^{3+})$ and $Yb^{3+}(Bi^{3+})$ was estimated by the integral absorption cross-section (in $cm^2\,cm^{-1}$) of the satellites with frequencies $\sim$10,200 $cm^{-1}$ (Mo) and $\sim$10,182 $cm^{-1}$ (Bi) (marked by a symbol of the element circled in Fig. 2).

| No | Sample | Solvent | $\sigma_{int}$ [$Yb^{3+}(Bi^{3+})$] | $\sigma_{int}$ [$Yb^{3+}(Mo^{3+})$] | Growth lab |
|---|---|---|---|---|---|
| 1 | $YAl_3(BO_3)_4$:Yb(7%) | $Bi_2Mo_3O_{12}$ | 7.5 | <1 | KIP |
| 2 | $YAl_3(BO_3)_4$:Yb(7%) | $Bi_2Mo_3O_{12}$ + 0.05 $Bi_2O_3$ | 26.2 | <1 | KIP |
| 3 | $YAl_3(BO_3)_4$:Yb(7%) | $Bi_2Mo_3O_{12}$ + 0.15 $MoO_3$ | <0.1 | 34 | KIP |
| 4 | $YAl_3(BO_3)_4$:Yb(10%) Tm(5%) | $Bi_2Mo_3O_{12}$ | 0.7 | <1 | KIP |
| 5 | $TmAl_3(BO_3)_4$:Yb(10%) | $Bi_2Mo_3O_{12}$ | <0.1 | 74 | KIP |
| 6 | $LuAl_3(BO_3)_4$:Yb(5%) | $Bi_2Mo_3O_{12}$ | 1.6 | 20 | KIP |
| 7 | $YAl_3(BO_3)_4$:Yb(4.5%) | $K_2Mo_3O_{10}$ | – | 61 | MSU |
| 8 | $YAl_3(BO_3)_4$:Yb(8%) | $K_2Mo_3O_{10}$ | – | 153 | UV |
| 9 | $YAl_3(BO_3)_4$:Yb(2.5%) | $K_2Mo_3O_{10}$ | – | 124 | UV |
| 10 | $YAl_3(BO_3)_4$:Yb(0.3%) | $K_2Mo_3O_{10}$ | – | 115 | UV |
| 11 | $YAl_3(BO_3)_4$:Yb(2%) | $K_2Mo_3O_{10}$ | – | 149 | LCMCP |
| 12 | $YAl_3(BO_3)_4$:Yb(5%) | $LaB_3O_6$ | – | – | LCMCP |

The bismuth–lithium–molybdenum based flux contained a mixture of $Bi_2Mo_3O_{12}$ and $Li_2MoO_4$ [12], 85 mass% of ($Bi_2Mo_3O_{12}$ + 0.5 $Li_2MoO_4$ + 2 $B_2O_3$) + 15 mass% of $R_{1-x}Yb_xAl_3(BO_3)_4$. This flux was prepared by melting at the temperatures 1000–1050 °C a mixture of $Bi_2O_3$, $MoO_3$, $Li_2CO_3$, $B_2O_3$, $R_2O_3$, $Yb_2O_3$, and $Al_2O_3$ powders in a proportion determined by the above formula. After growing the single crystal with x = 0.07 (**1** in Table 1), a suitable amount of $Bi_2O_3$ was added into the remaining flux and crystallization was repeated. The crystal **2** was obtained (Table 1). Then, a suitable amount of $MoO_3$ was added to the residual flux and crystallization was repeated again (**3** in Table 1). In Table 1, these fluxes are denoted as ($Bi_2Mo_3O_{12}$), ($Bi_2Mo_3O_{12}$ + 0.05 $Bi_2O_3$), and ($Bi_2Mo_3O_{12}$ + 0.15MoO), respectively. Single crystals with dimension up to 10 × 12 × 12 $mm^3$ were grown on seeds. A high optical quality was achieved at the growth rates not exceeding 0.5 mm per day.

The complex solvent containing potassium trimolybdate $K_2Mo_3O_{10}$ with an excess of boron and rare earth oxides was used for $YAl_3(BO_3)_4$:Yb crystallization carried out at Moscow State University (MSU) (sample **7**) [13]. Starting chemicals (at least 99.99% and 99.999% purity for rare earths and other materials, respectively) were $Y_2O_3$, $Yb_2O_3$, $Al_2O_3$, and $B_2O_3$ but $K_2Mo_3O_{10}$ was previously sintered from $K_2MoO_4$ and $H_2MoO_4$ at 650 °C according to the reaction: $K_2MoO_4 + 2H_2MoO_3 = K_2Mo_3O_{10} + 2H_2O\uparrow$. The starting charge was mixed, placed into a platinum crucible, and homogenized at 1150 °C in a high-temperature furnace for 24–48 h. The temperature at the bottom of the crucible was kept 2–3 °C higher than at the melt surface. The single crystal of $Y_{0.955}Yb_{0.045}Al_3(BO_3)_4$ (sample **7**) was obtained by dipping seeded solution growth (DSSG) method. The fraction of YAB:Yb crystalline substance in the starting solutions was 17 wt.%. Before DSSG, the saturation temperatures of fluxed melts were determined by a probe technique as 1060–1080 °C. A "point" YAB seed of 0.3 × 0.3 × 1.0 $mm^3$ size was dipped into fluxed melt. During the crystal growth, supersaturation was kept within the temperature range 1080–1000 °C by cooling of fluxed melts at a rate 0.2–5 °C/day following the experimental data on the solubility and crystallization kinetics. At the end of the growth process, the crystal was pulled out and cooled to room temperature within several days.

In the University of Verona, a flux containing a mixture of $K_2SO_4$ and $MoO_3$ in the molar ratio 1:3 was used [14]. Appropriate amounts of $Y_2O_3$, $Al_2O_3$, $B_2O_3$, and $Yb_2O_3$ were mixed with the solvent. The ratio of the crystal components to the solvent was 40:60 (wt.%). The mixtures were heated to 1120 °C at 300 °C/h, kept at this temperature for 3 h, and then slowly cooled down to 850 °C with a rate of about 1 °C/h. Upon removing the solvent by boiling in concentrated KOH, hexagonal rods up to 5 × 3 × 3 $mm^3$ were obtained. While the largest crystals clearly contained solvent inclusions, smaller crystals (about 2 × 1 × 1 $mm^3$) were reasonably

clear and transparent and only those were used for the optical measurements (crystals **8–10**).

The Yb-doped YAB crystals **11** and **12** were grown in the LCMCP. The crystal **11** was obtained as described in Ref. [15], using the $K_2Mo_3O_{10}$ based flux. The solvent was made from 40 mol.% KF and 60 mol.% $MoO_3$ and mixed with oxides to prepare YAB. The ratio of the crystal components to the solvent was 27:73 mol.%. 130 g of the oxide-solvent mixture was introduced into a 50 $cm^3$ platinum crucible capped with a platinum foil and then allowed to a slow cooling from 900 °C down to 700 °C at 2 °C/h. The second crystal (**12** in Table 1) was grown using a mixture of $Y_{0.95}Yb_{0.05}Al_3(BO_3)_4$ and $LaB_3O_6$ in molar ratio 1:2. The mixture was prepared from reagent grade binary oxides, put into a platinum crucible, heated up to 1200 °C, and then cooled down at a rate 1 °C/h to get the primary crystallization of YAB:Yb.

Polarized absorption spectra were measured at 3.5 K using a high-resolution Fourier-transform spectrometer Bruker IFS 125 HR with a Si detector (for the visible spectral region) or photomultiplier (for the UV spectral region) and a closed-cycle cryostat Cryomech ST403. The resolution for the absorption measurements was up to 0.1 $cm^{-1}$ and was chosen to reproduce correctly the narrowest details in the spectra. The spectra were registered in the $\alpha$ (**k**||$c$, **E**, **H** $\perp c$), $\sigma$ (**k**$\perp c$, **E**$\perp c$), and $\pi$ (**k**$\perp c$, **E**||$c$) polarizations.

The element composition of the samples was controlled by optical emission spectroscopy (OES) using a Papuas 4DI OES spectrometer designed and fabricated in the Institute of Spectroscopy (Russian Academy of Sciences). A sample was ground into powder, mixed with pure carbon (graphite), and this mixture was used as an electrode. The electric arc passing through the prepared mixture excited atoms and this allowed observing the atomic spectral lines. We analyzed spectra in the range from 240 to 410 nm with a spectral resolution of 0.09 nm. This method is very sensitive but not precise when determining the absolute values of the concentration of the elements.

## 3. Results and discussion

The low-temperature $\sigma$-polarized spectra of different Yb-doped rare-earth aluminum borates are presented in Fig. 1. The spectra agree with the previously published spectra of YAB:Yb [11,16] and YbAB [17] crystals. On the high-frequency side of the purely electronic zero-phonon lines 0–0′, 0–1′, and 0–2′ vibronic bands are observed, due to the interaction of electronic levels of ytterbium with lattice vibrations. Vibronic bands in the spectra of the YbAB crystals were studied in our earlier paper [18], where a comparison was made with infrared and Raman spectra as well. The vibronic structure differs markedly in RAB:Yb crystals with different R ions, which is, evidently, caused by differences in the phonon
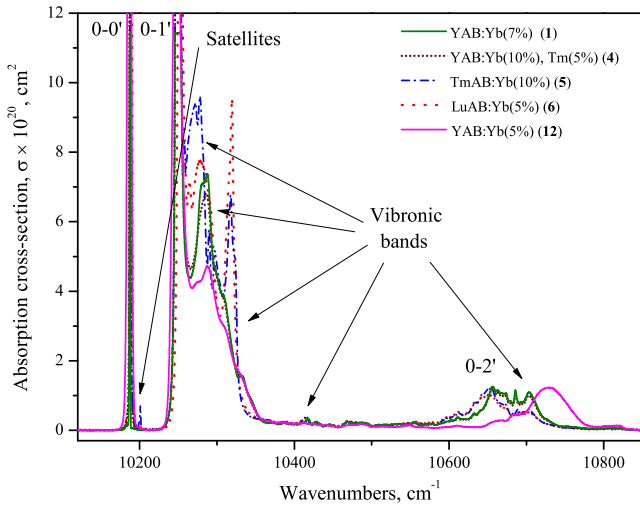
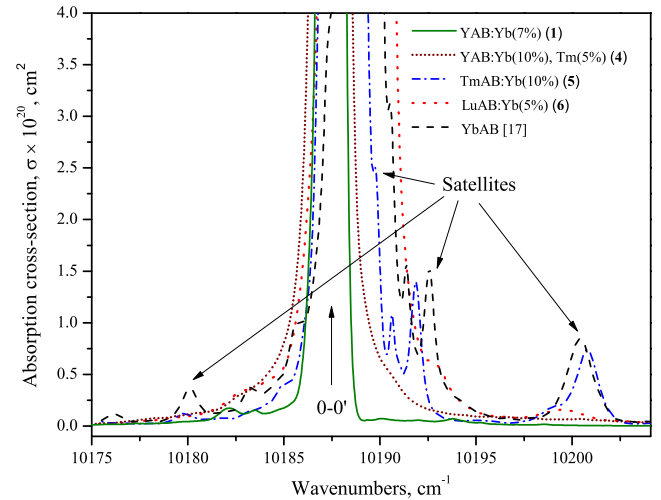**Fig. 1.** Absorption spectra of $Yb^{3+}$ in different $R$AB:Yb single crystals.



**Fig. 2.** Zero-phonon line $0(^2F_{7/2}) \rightarrow 0'(^2F_{5/2})$ of $Yb^{3+}$ in $R$AB single crystals doped with $Yb^{3+}$. Numerous satellites are observed.

spectra of these crystals. More detailed conclusions would be possible after studying the phonon spectra of these crystals which is out of the scope of the present paper.

Near the main electronic line 0–0′, many additional weak and narrow lines (satellites) are observed in the spectra of all the crystals, similarly as for the spectra of previously studied YbAB [17] and YAB:Yb [11] crystals. In Refs [11,17], we assumed that the satellites are connected with the absorption of the $Yb^{3+}$ ions in regular crystal lattice positions but with defects in the nearest surrounding. These defects might be elements of the solvent that enter into positions of the regular ions in the crystal lattice during crystallization. From a comparison of the ionic radii of rare-earth ions in the sixfold coordination [19] ($r(Lu^{3+}) = 0.861$ Å, $r(Yb^{3+}) = 0.868$ Å, $r(Tm^{3+}) = 0.88$ Å, $r(Y^{3+}) = 0.9$ Å) and aluminum ($r(Al^{3+}) = 0.535$ Å), on the one hand, and bismuth ($r(Bi^{3+}) = 1.03$ Å) and Mo ($r(Mo^{3+}) = 0.69$ Å), on the other hand, we have suggested a hypothesis that bismuth enters into the position of the rare-earth ion but molybdenum enters into the position of aluminum [11,17]. Such defects induce local deformations of the crystal lattice, which lead to a shift of spectral lines of the $Yb^{3+}$ ions nearest to these defects, $Yb^{3+}(Bi^{3+})$ and $Yb^{3+}(Mo^{3+})$

(and to a broadening of the lines of more distant ions). Fig. 2 shows these satellites for different rare-earth aluminum borates doped with the $Yb^{3+}$ ions.

Fig. 3 shows that the satellite lines in the spectra of the YAB:Yb single crystals **1–3** (grown from flux based on $Bi_2Mo_3O_{12}$) and **8** (grown from flux based on $K_2Mo_3O_{10}$), which have similar concentration of $Yb^{3+}$ ($x = 0.07$–$0.08$), differ significantly. The integrated intensity of the satellite lines and, therefore, the concentration of non-equivalent $Yb^{3+}$ centers is much smaller in the crystals **1–3** grown from the $Bi_2Mo_3O_{12}$ based fluxes than in the crystals **7–11** grown with the $K_2Mo_3O_{10}$ based ones. This points to a stronger incorporation of the Mo impurities into a crystal grown with the latter flux.

It could be expected that an addition of $Bi_2O_3$ into the flux **1** results in an increase of the concentration of the $Yb^{3+}(Bi^{3+})$ centers and in an increase of the intensity of corresponding satellite lines. Indeed, some of the satellite lines in the absorption spectrum of the crystal **2** grown with an excess of Bi are more intense than in the spectrum of the stoichiometric crystal **1** (see Fig. 3). The satellite lines whose intensity increases with increasing content of bismuth
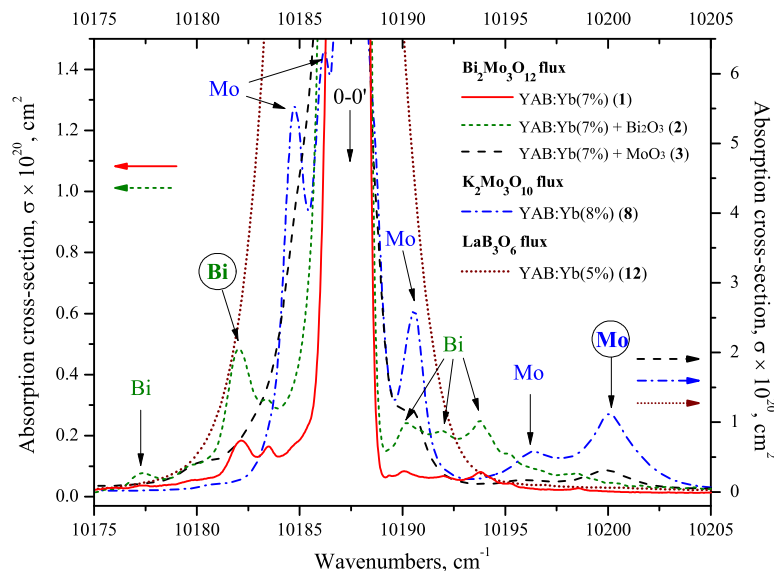


**Fig. 3.** Zero-phonon line $0(^2F_{7/2}) \rightarrow 0'(^2F_{5/2})$ of $Yb^{3+}$ in YAB single crystals doped with $Yb^{3+}$ in similar concentrations but grown using different solvents.
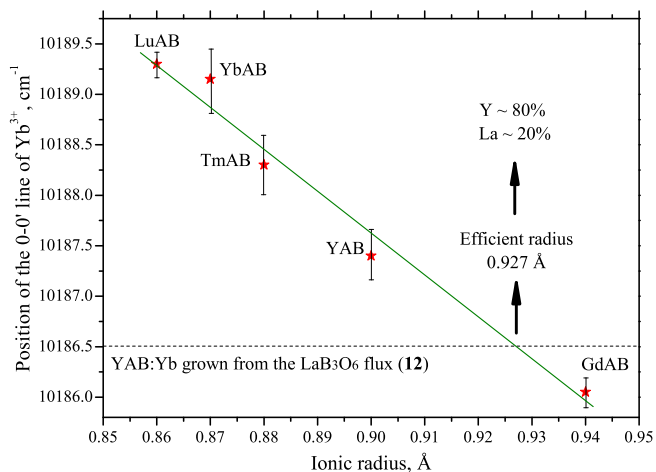
**Fig. 4.** The frequency of the absorption line 0–0′ of the $Yb^{3+}$ ion as a function of ionic radius of the main rare-earth ion $R^{3+}$ in the $R$AB:Yb crystals.



**Fig. 5.** OES spectra of YAB single crystals doped with $Yb^{3+}$ in similar concentrations and grown from different fluxes.

in the flux can unambiguously be ascribed to the $Yb^{3+}$($Bi^{3+}$) centers. A similar situation is observed when adding the molybdenum oxide over the stoichiometry of $Bi_2Mo_3O_{12}$. Satellite lines of the $Yb^{3+}$ ($Mo^{3+}$) centers appear in the absorption spectrum of the crystal **3** grown with an excess of Mo (Fig. 3). A simple explanation of these results is as follows. When preparing the flux based on $Bi_2Mo_3O_{12}$ + 0.5 $Li_2MoO_4$ the initial components for $Bi_2Mo_3O_{12}$ were $Bi_2O_3$ and $MoO_3$. A small part of $MoO_3$ is lost because of its high volatility. Thus, the prepared flux has an excess of $Bi_2O_3$. The single crystal **1** was grown from such flux. The single crystal **2** was grown from flux which has a higher content of unbound $Bi_2O_3$. But $MoO_3$ evaporates quickly, and therefore has a small influence on the processes in the boundary layer. In fact, the single crystal **3** was grown from the flux with the lowest amount of $Bi_2O_3$ (see Fig. 3). A useful technical advice follows from the above description: when preparing the fluxes on the basis of $Bi_2Mo_3O_{12}$ it is better to use $Bi_2Mo_3O_{12}$ than a mixture of powders $Bi_2O_3$ and $3MoO_3$. Fig. 3 shows that the satellite lines due to the $Yb^{3+}$($Mo^{3+}$) centers are very strong in the case of $K_2Mo_3O_{10}$ based flux (the crystal **8**). Table 1 summarizes the results on the absorption cross-section for the $Yb^{3+}$($Bi^{3+}$) and $Yb^{3+}$($Mo^{3+}$) centers in the studied crystals.

In single crystals with a double doping, e.g. in $Y_{1−x−y}Yb_xTm_yAl_3$ $(BO_3)_4$ ($x \ll 1$, $y \ll 1$) which are interesting for laser schemes based on $Tm^{3+} \leftrightarrow Yb^{3+}$ energy transfer, along with distorted rare-earth centers generated by the Bi- and Mo- impurities also the $Yb^{3+}$ ($Tm^{3+}$) centers should exist. However, $Yb^{3+}$ and $Tm^{3+}$ have very similar ionic radii so that the perturbation will be very small.

We have also analyzed the $Yb^{3+}$($Mo^{3+}$) centers in the crystals grown independently in different laboratories by the same method using the $K_2Mo_3O_{10}$ based flux. The results are presented in Table 1. One can see that the concentration of Mo impurity is very different, presumably owing to the different growth conditions. Thus, our spectroscopic method allows to define the quality of the ytterbium doped aluminum borate single crystals. This method gives the possibility to study the influence of the growth conditions on the quality of crystals, allowing the improvement of the growth technique.

As for the crystals grown from the flux based on $LaB_3O_6$, they obviously do not contain impurities like molybdenum and bismuth. The lanthanum is the only possible impurity in such crystals. Indeed, we did not find spectral satellites in the vicinity of the main line 0–0′ of $Yb^{3+}$. The latter, however, was broader and demonstrated a frequency shift in comparison with other investigated crystals. Our study has evidenced that in the rare-earth aluminum borate crystals doped with ytterbium, the position of the electronic
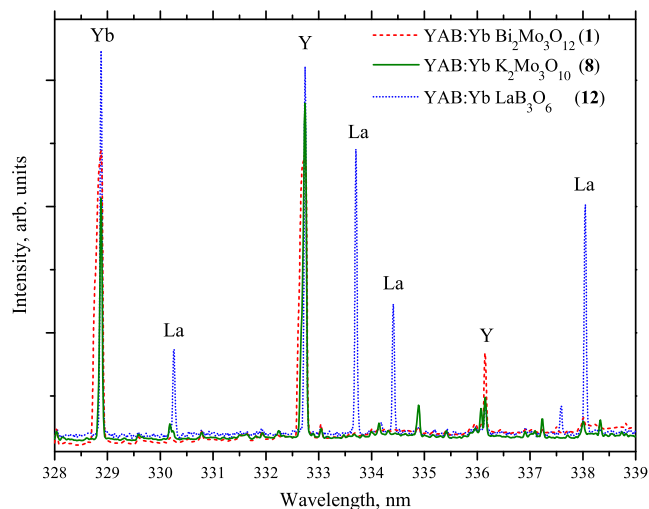
line 0–0′ of the $Yb^{3+}$ ion depends on the main rare-earth ion (Lu, Yb, Tm, Y, Gd). Fig. 4 shows the frequency of the $Yb^{3+}$ 0–0′ line in the $R$Al$_3$(BO$_3$)$_4$:Yb crystals as a function of the ionic radius of the main $R^{3+}$ ion. These points are quite well approximated by a straight line. The position of the 0–0′ line in the YAB:Yb crystal grown using the $LaB_3O_6$ as a solvent (**12** in Table 1) indicated by a dashed line, did not coincide with the position of 0–0′ line in $R$AB crystals. From the point of intersection of the dashed line and the approximating line we have found that the effective ionic radius for this compound is 0.927 Å, which corresponds to 20% lanthanum substitution for yttrium ions. This explains the appearance of a large inhomogeneous broadening of the electronic lines of ytterbium in these crystals. The OES analysis has shown a significant concentration of lanthanum in the sample **12** (see Fig. 5), which is in favor of our conclusions.

Finally, we analyzed the transmission spectra in the ultraviolet spectral region of YAB:Yb crystals grown by different methods. Both pure and Yb-doped crystals were studied. We have found that the presence of the $Yb^{3+}$ ions does not shift the observed UV
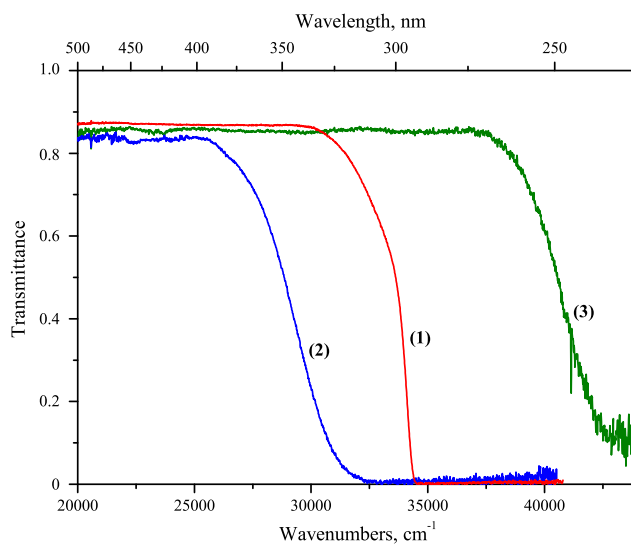


**Fig. 6.** Transmission at room temperature in the visible-ultraviolet spectral region of 0.20 mm thick YAB:Yb single crystals grown from fluxes based on (1) $Bi_2Mo_3O_{12}$ (sample **1**), (2) $K_2Mo_3O_{12}$ (sample **11**), (3) $LaB_3O_6$ (sample **12**).

absorption edge, which is in agreement with the data of Ref. [20]. According to Ref. [20], the $Yb^{3+}$ charge-transfer absorption band in similar borates is located at about 200 nm, i.e. above the observed absorption edge in our YAB crystals. Fig. 6 shows that the YAB:Yb crystals grown from the $K_2Mo_3O_{10}$-based flux and, thus, containing large concentration of the Mo impurity are not transparent above $\sim$30,000 $cm^{-1}$ (330 nm). For the crystals grown from the $Bi_2Mo_3O_{12}$-based flux, the UV absorption edge shifts to $\sim$34,000 $cm^{-1}$ (295 nm), while the crystal grown using the $LaB_3O_6$ solvent is transparent up to 42,000 $cm^{-1}$ (240 nm). This makes the last solvent the most promising for growing rare-earth aluminum borates with improved transparency in the UV region.

## 4. Conclusions

Study of the fine structure of absorption spectra of the $R_{1-x}Yb_xAl_3(BO_3)_4$ crystals grown from bismuth–lithium molybdate $(Bi_2Mo_3O_{12})$ based flux and potassium molybdate $(K_2Mo_3O_{10})$ based flux allows identifying the spectral satellites in the vicinity of the main 0–0′ line of $Yb^{3+}$. They are due to optical transitions of $Yb^{3+}$ having either molybdenum or bismuth impurity in the nearest surrounding, $Yb^{3+}(Mo^{3+})$ and $Yb^{3+}(Bi^{3+})$. We show that the concentration of the molybdenum impurity (the main factor shifting the UV absorption edge to larger wavelengths) is more than an order of magnitude higher in YAB crystals grown with the $K_2Mo_3O_{10}$ solvent, as compared to the crystals grown with the $Bi_2Mo_3O_{12}$ solvent. Moreover, this concentration depends not only on the solvent used but also on the growth conditions. We also show that the crystals grown with the $LaB_3O_6$ solvent contain a significant amount of the lanthanum impurity (which induces a broadening of the rare-earth spectral lines) but, among the studied samples, are the most transparent in the UV spectral region.

To summarize, our spectroscopic method can be used for a rapid analysis of YAB crystals and for the improvement of the growth technique of these crystals.

## References

[1] D.N. Nikogosyan, Nonlinear Optical Crystals: A Complete Survey, Springer, Berlin, 2005. p. 427.
[2] N.I. Leonyuk, L.I. Leonyuk, Progr. Cryst. Growth Charact. 31 (1995) 179.
[3] D. Jaque, J. Alloys Compd. 204 (2001) 323.
[4] A. Brenier, C. Tu, Z. Zhu, B. Wu, Appl. Phys. Lett. 84 (2004) 2034.
[5] P. Wang, J. Dawes, P. Dekker, J. Piper, Opt. Comm. 174 (2000) 467.
[6] H. Jiang, J. Li, J. Wang, X-B. Hu, H. Liu, B. Teng, C-Q. Zhang, P. Dekker, P. Wang, J. Cryst. Growth 233 (2001) 248.
[7] P. Burns, J. Dawes, P. Dekker, J. Piper, J. Li, J. Wang, Opt. Comm. 207 (2002) 315.
[8] G. Dominiak-Dzik, W. Ryba-Romanowski, R. Lisiecki, I. Foldvári, E. Beregi, Opt. Mater. 31 (2009) 989.
[9] A.S. Aleksandrovsky, I.A. Gudim, A.S. Krylov, A.V. Malakhovskii, V.L. Temerov, J. Alloys Compd. 496 (2010) L18.
[10] X. Yu, Y. Yue, J. Yao, Z. Hu, J. Cryst. Growth 312 (2010) 3029.
[11] K.N. Boldyrev, M.N. Popova, L.N. Bezmaternykh, M. Bettinelli, Quant. Electron. 41 (2011) 120.
[12] V.L. Temerov, A.E. Sokolov, A.L. Sukhachev, A.F. Bovina, I.S. Edelman, A.V. Malakhovskii, Cryst. Rep. 53 (2008) 7.
[13] N.I. Leonyuk, V.V. Maltsev, E.A. Volkova, E.V. Koporulina, N.V. Nekrasova, N.A. Tolstik, N.V. Kuleshov, J. Phys.Conf. Series 176 (2009) 012010.
[14] M.H. Bartl, K. Gatterer, E. Cavalli, A. Speghini, M. Bettinelli, Spectrochim. Acta Part A: Mol. Biomol. Spectrosc. 57 (2001) 1981.
[15] G. Aka, N. Viegas, B. Teisseire, A. Kahn-Harari, J. Godard, J. Mater. Chem. 5 (4) (1995) 583.
[16] M. Ramírez, L. Bausá, D. Jaque, E. Cavalli, A. Speghini, M. Bettinelli, J. Phys.: Condens. Matter 15 (2003) 7789.
[17] M.N. Popova, K.N. Boldyrev, P.O. Petit, B. Viana, L.N. Bezmaternykh, J. Phys.: Condens. Matter 20 (2008) 455210.
[18] K.N. Boldyrev, B.N. Mavrin, M.N. Popova, L.N. Bezmaternykh, Opt. Spectrosc. 111 (2011) 420.
[19] R.D. Shannon, Acta Cryst. A32 (1976) 751–767.
[20] L. van Pieterson, M. Heeroma, E. de Heer, A. Meijerink, J. Lum. 91 (2000) 177.